ELSEVIER

Materials Science and Engineering A 418 (2006) 223–228

MATERIALS SCIENCE & ENGINEERING A

www.elsevier.com/locate/msea

Microstructure of surface composite Al_2O_3/Ni on copper substrate produced by vacuum infiltration casting

Gui-rong Yang [a,*], Wen-ming Song [a], Jin-jun Lu [b], Yuan Hao [a], Ya-min Li [a], Ying Ma [a]

[a] *State Key Laboratory of New Nonferrous Metal Materials, School of Materials Science and Engineering, Lanzhou University of Technology, Lanzhou 730050, Gansu, China*

[b] *State Key Laboratory of Solid Lubrication, Lanzhou Institute of Chemical Physics, Chinese Academy of Sciences, Lanzhou 730000, Gansu, China*

Accepted 21 November 2005

Abstract

This present work reports on the microstructure and hardness of infiltrated Al_2O_3/Ni layers on the copper substrate. The infiltrated layer was produced by vacuum infiltration casting technique (VICT) using Ni-based powder and Al_2O_3 particulates with different content. By optimizing the processing parameters, a compact infiltrated layer is achievable as confirmed through SEM observation. The infiltrated layer is composed of surface composite layer and transition layer, and the thickness of the transition layer decreases with the increasing content of Al_2O_3. The hardness of the surface composite has been evaluated. The macro-hardness of the layer is about HRC 65.0 and the distribution of micro-hardness shows a gradient change. The average micro-hardness of the infiltrated layer is about HV700.

Keywords: Al_2O_3/Ni surface composite; Vacuum infiltration casting; Copper substrate; Gradient structure; Hardness

1. Introduction

Alumina has a relatively high melting point (2045 °C) and boiling temperature (2980 °C), while copper has an extremely high thermal (400 W m^{-1} K^{-1}) and electrical conductivity of 100% IACS (International annealed copper standard) [1]. Therefore, copper-matrix composite reinforced by alumina particulate has been considered one of the best candidates for a variety of applications, including its use as electrical contact materials and heat conductor materials [1–5]. So far, many methods have been employed to fabricate alumina particulate reinforced copper-matrix composite by stirring casting and powder metallurgy (PM), such as sintering, internal oxidation, mechanical alloying, and pressureless infiltration [6–9]. The use of surface composite opens up the possibility for material designs in which the specific properties are located where they are most needed [10]. The substrate material can be designed for strength and toughness, while the surface composites are responsible to wear, thermal loads and corrosion [11–13].

A variety of methods for producing surface materials (coating) on copper substrate, such as electro-plating, chemical-plating, physical vapor deposition and heat treatment, have recently been developed [14–16]. The fabrication of surface layer on copper substrate proves to be a tough job compared to the use of steel or iron substrate because of its excellent heat conductivity. The surface layer produced through these methods is not more than 100 μm in thickness [14–17]. Infiltration casting technique is a novel process for producing surface materials [18]. It takes potential advantages to achieve a near-net shape product in a simple and cost effective manner, widely select the matrix, and have good bonding between the surface layer and substrate or the bonding between the particulates and the matrix.

In this study, the surface composites Al_2O_3/Ni on copper substrate were fabricated by the vacuum infiltration casting technique (VICT). The present article deals with the micro-structural aspects of the infiltrated layer and the study of hardness of the surface layer.

2. Experimental procedures

2.1. Fabrication of infiltrated layers

In this work, bronze ZQAl9-4 was chosen as matrix of the surface composite layer and the substrate material on which the infiltrated layer was formed. The selected copper alloy has been

* Corresponding author. Tel.: +86 931 2973640; fax: +86 931 2755806.
E-mail address: yanggrming@lut.cn (G.-r. Yang).

0921-5093/$ – see front matter © 2005 Elsevier B.V. All rights reserved.
doi:10.1016/j.msea.2005.11.029

Table 1
The chemical composition of tested aluminum bronze (wt.%)

Cu	Balance
Al	8.0–10.0
Fe	2.0–4.0
Sb	≤0.05
Si	≤0.2
P	≤0.1
As	≤0.05
Sn	≤0.2
Pb	≤0.1
Mn	≤0.5
Zn	≤1.0
Total	≤1.0

widely used in applications, such as machine, mine, spaceflight parts and electronic [1–5]. Table 1 gives its chemical composition [19]. The Ni-based alloy powder consists of Ni-based solid solution, boride and Ni–Cr alloy [20,21]. The surface layer containing these hard phases can be applied in the circumstances of wear, erosion and oxidation-resistance. They might be used at these conditions of air corrosion, seawater, steam and weak acid. Ni-based alloying powder and Al_2O_3 powder with different ratios were chosen as the raw materials for producing the surface composites. The Al_2O_3 particulates coated with Ni-layer (several nm in thickness) were commercially available from Beijing Nonferrous Metal Institute to prompt the wettability between bronze melt and the Al_2O_3 particulates.

The surface infiltrated layer was fabricated by a vacuum infiltration casting process. First, the preform layers with different alumina contents were prepared, as listed in Table 2. The combined powders and self-fabricated binder (NJB, its main components are boric acid and latex) were mixed together according to desired proportion, paved on the inner surface of a casting mould or outer surface of mould cores, where the characteristic were needed to improve, then heated to harden so as to form preform layer. Second, the melt of bronze was poured at 1220 °C into the mould in vacuum. By sucking force of the vacuum degree, the melt was sucked into the preform, and the surface infiltrated layer was obtained after solidification. The fabrication principle is shown in Fig. 1.

2.2. Evaluation of the microstructure

The specimens of the surface layers for micro-structural observation were cut out along the direction from infiltrated layer surface to substrate, ground and polished using standard metallographic techniques. The microstructure of surface infiltrated layer obtained was examined by scanning electron microscope (SEM) of HITACHI S-520. The distribution of elements was analyzed by EPMA-1600. The phases were determined by an X-ray diffractometer (D/mac-rc) in the range of 20–100°at the speed of 4°/min.

Table 2
The weight fraction of powder used infiltration experiment

Code of the combined powder	Composition of the combined powder (wt.%) (200–320 mesh)	
	Al_2O_3 powder	Ni-based alloying powder
A	10	90
B	20	80
C	30	70
D	40	60

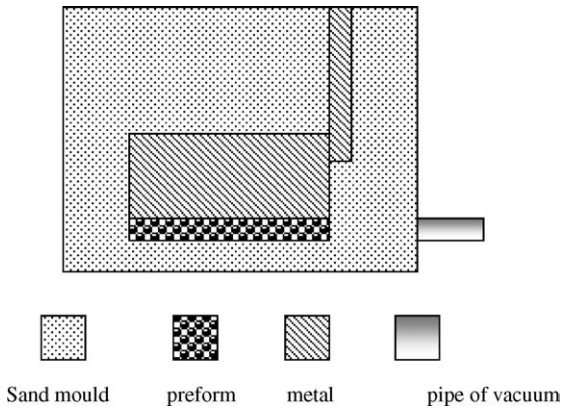

Fig. 1. The sketch of set-up for forming infiltrated layer.

2.3. Hardness measurements

The macro-hardness was measured using HRS-150 Rockwell hardness tester. The normal load was 1471 N and loading time was 5 s. The micro-hardness was measured using MH-5 microhardness tester at the load of 9.8 N and loading time of 10 s.

3. Results and discussion

3.1. Microstructure of infiltrated layer

The thickness of the infiltrated layer fabricated through vacuum infiltration casting technique (VICT) is 2–2.5 mm. Fig. 2 shows the typical microstructure of the surface infiltrated composite layer prepared by the vacuum infiltration casting technique. The content of Al_2O_3 among the surface composite is 10%. Fig. 2a shows the cross-sectional view of the infiltrated layer. The Al_2O_3 particulates are uniformly distributed in the matrix. The micrographs reveal continuous and sound interfaces between the substrate and the infiltrated layer and no crack could be found. No spalling or separation is appeared even at high magnification. Fig. 2b shows the transition layer between the surface composite and the substrate. The diffusion layer was about 100–150 μm in thickness. Fig. 2c shows the microstructure of the surface composite corresponding to spot A in Fig. 2a. Ni-based solid solution with Ni_3B, $Ni_{31}Si_{12}$ and β phase of Ni–Cr alloy or Ni–Si alloy dispersed among the Ni matrix was found. It shows that the microstructure of outer layer is sound. This is the microstructure of the Ni matrix. Spot B in Fig. 2d is the interface of particle and matrix. The peeling off of the particle happened during the preparation of the polished sample due to hardness difference of Al_2O_3 and the Ni matrix. Fig. 3 represents the microstructure of surface composites with different content of Al_2O_3. It shows that the distribution of particulates

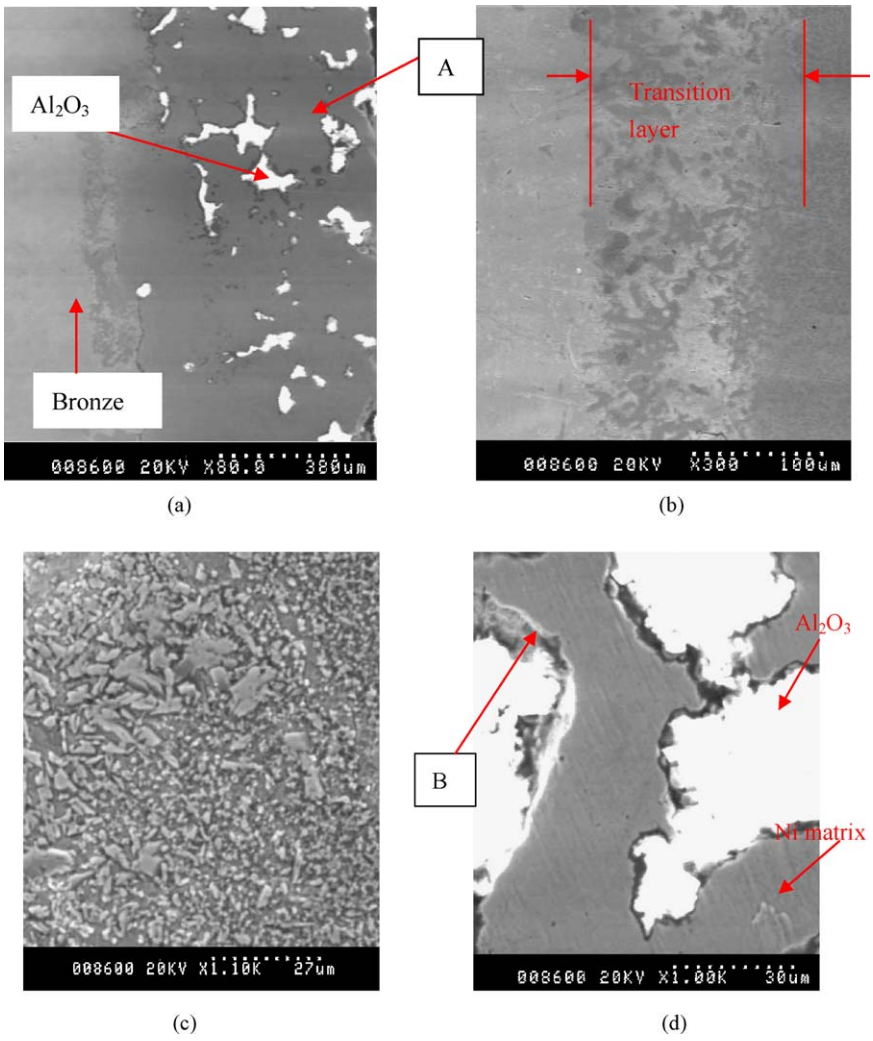

Fig. 2. The SEM view of infiltrated layer (the content of Al_2O_3 is 10%).

is very uniform. The pits of the surface were formed during the preparation of metallographic specimens.

The formation of the infiltrated layer is semi-metallurgical fusion because the melting point ($1000 \pm 50\,^{\circ}C$) of Ni-based alloying powder is lower than that of copper alloy, while the Al_2O_3 could not melt. After pouring the melt, the metal penetrated into the pores and capillaries of preform and went through all the preform to the outer preform close to the mould surface.

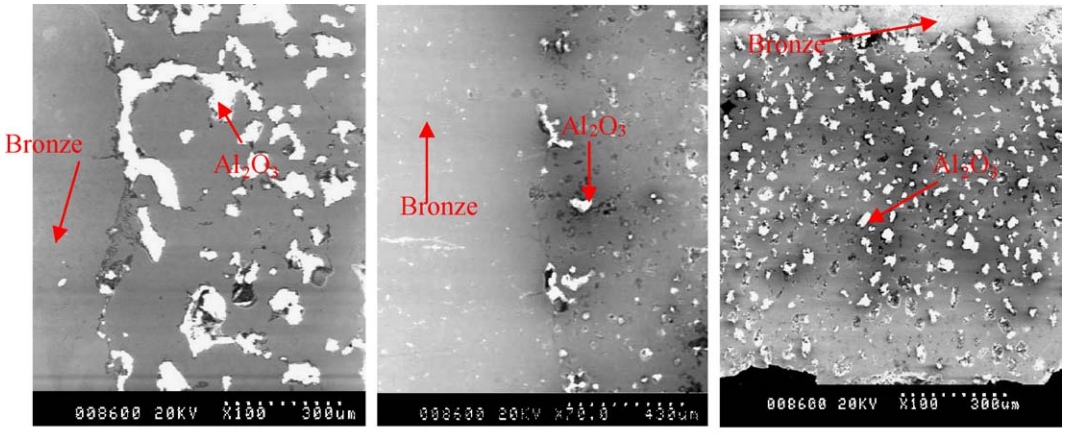

Fig. 3. The SEM view of surface composite with different content of Al_2O_3.

The energy loss of copper melt is higher than that of the inner owing to the chilling action of mould and perform. Therefore, the time of copper in a molten state to solid state is shorted markedly The Ni-based alloying powder melted as the melt of bronze went through the perform. However, the heat exchange between the alloying powder and the melt of bronze was not high enough to activate the atom diffusion. Consequently, the Ni-based powder melted only at the original place, and then solidified with copper alloy. So the Al_2O_3 particulates were not moved, while the Ni on the surface of Al_2O_3 particle fused with the Ni-based powder melt and the copper melt to form the surface composite Al_2O_3/Ni. The microstructure of surface composite is shown in Fig. 2. The microstructure of the most outer layer was soundness though the time of keeping melt state was short compared to that of the inner layer seen from Fig. 2c. The outer surface composite layer is mainly composed of a Ni-based alloy, Al_2O_3 and a little fraction of copper. The initial temperature of melt is always 1220 °C and less chilling effect due to preheating more time for formation of transitional layer. The Ni-based alloying powder could obtain enough energy to form the transition layer with copper alloy. The Ni-based alloying powder can melt and the atoms of the alloying powder can diffuse within close distance only to form many active atoms that may infiltrate directly into the substrate to form solid solution in the advantageous place. With the increasing content of Al_2O_3, the transition layer became thinner. The thickness of transition layer is about 30–70 μm for infiltrated layer with Al_2O_3 content being more than 30%. The fraction of Ni-based self-fusion powder decreased with the increasing content of Al_2O_3. The content of coated Ni-layer surrounding the Al_2O_3 particulates increased. The powders in preform have to absorb energy from the melt of bronze to form the surface composite. The melting point of Ni is 1453 °C and that of Ni-based powder is 1000 ± 50 °C. The Al_2O_3 particulates need more energy from the melt of bronze to fuse with the Ni-based alloy. So with the increasing content of the Al_2O_3, the Al_2O_3 particulates would absorb more energy to forming soundness surface composite layer. The energy that Ni-based powder absorbed would decrease. The number of active atoms forming transition layer decreased and its diffusion capability dropped, too.

Distributions of Ni, Cr, Cu across the substrate and infiltrated layer are clearly shown in Fig. 4a, and the distribution of these elements is continuous. The concentrations of Ni and Cr gradually decreased at the joint of transition layer and substrate. On the other hand, the distribution of Cu increased gradually from the transition layer to substrate. The total layer thickness of the surface composite and the transition layer is larger than that obtained through the plating, heat treatment and vapor deposition because the preform can be prepared thicker and the resistance of diffusion in the liquid is small and the wasting energy is much less so that the distance of diffusion is long [22–24]. The temperature of diffusion of other methods, such as heat treatment, is lower than that of infiltration casting technique because the diffusion of atoms happens within solid for heat treatment. The structure of the infiltrated surface material is promising from the point of view of microstructure of structural materials as characterized by the transition layer. Combining Figs. 4 and 5, the following conclusions can be drawn. (1) The surface composite layer is composed of Al_2O_3, $Ni_{31}Si_{12}$ and Ni_3B ceramic particle and intermetallic compound, along with Ni–Cr–Fe alloy, Ni (Cr) solid solution and Ni (Cu) solid solution. (2) The transition layer is composed of Ni (Cr) solid solution, Ni (Cu) solid solution, Cu (Ni) solid solution and Ni–Cr–Fe alloy. The Ni–Cr–Fe alloy is too small in quantity to detect by XRD.

3.2. Hardness and bending behavior

3.2.1. The macro-hardness

The hardness of the copper substrate is around HRB 130. The hardness of infiltrated layer can reaches about HRC 65. The hardness of the infiltrated layer has been improved significantly. The main reason of increasing hardness is the Ni-based alloy reinforced by all kinds of hard phases mentioned above.

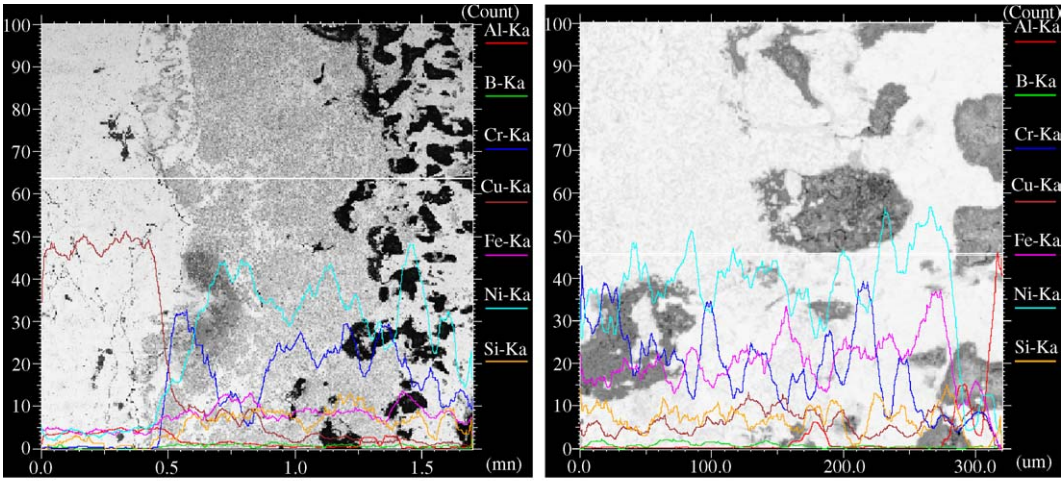

(a) Across infiltrated layer (b) Part of the composite

Fig. 4. The element distribution of infiltrated layer.

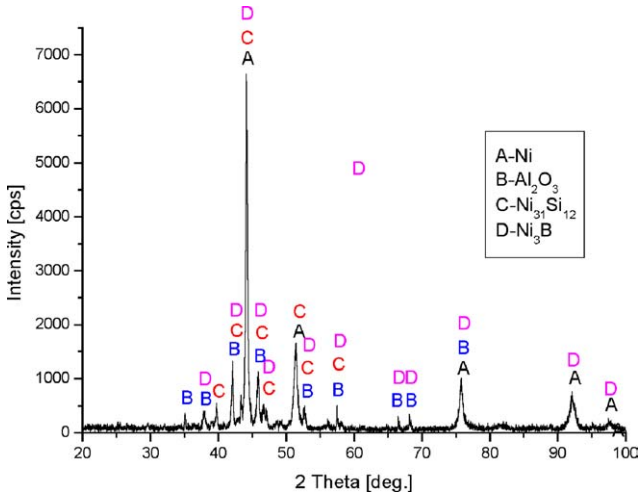

Fig. 5. XRD of infiltrated layer.

3.2.2. *The micro-hardness*

The distribution of all kinds of elements has been known from mentioned before as in Fig. 5. The concentration of Ni and Cr is high in the outer layer. The concentration of Ni and Cr decreases gradually from outer layer to substrate. The element Cr is less present than Ni in the transition layer because the diffusion coefficient of Cr is smaller than that of Ni [25,26]. So the diffusion of Cr in infiltrated layer could not be observed.

Fig. 6 shows the variation of micro-hardness with depth in the infiltrated layer. All infiltrated layers with different Al_2O_3 content show similar trend against depth. The highest value of hardness increases with the increasing content of Al_2O_3. The transition layer among infiltrated layer with Al_2O_3 content of 10% and 20% (100–150 μm) was thicker than that of 30% and 40% (30–70 μm). Therefore, the decrease of micro-hardness with Al_2O_3 content of 30% and 40% was quicker than that of 10% and 20% at the interface of surface composite and substrate. In the outer layer near the casting mould encountered unavoidable shrinkage porosity because chilling effect leads to

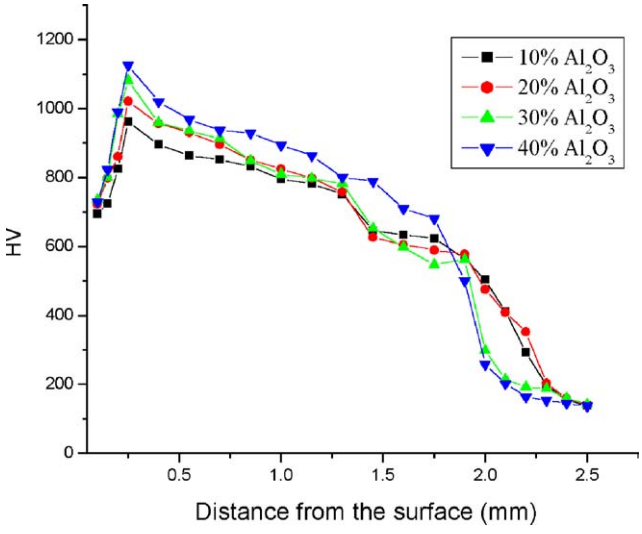

Fig. 6. The variation of micro-hardness across the infiltrated layer.

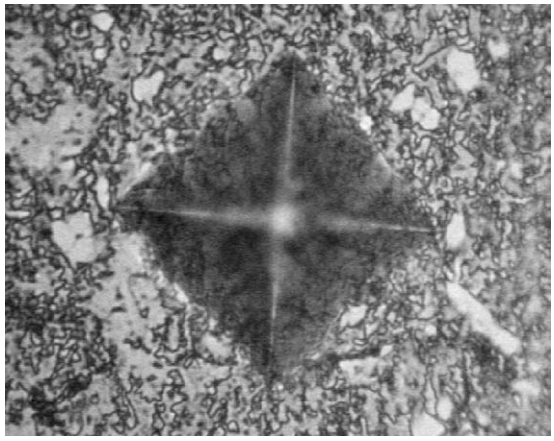

Fig. 7. The view of indentation.

un-perfect fusion. The compactness of outer layer is not as good as that of sub-surface layer, and therefore the hardness of the most outer layer is not the highest. The hardness reaches the highest value at the sub-surface layer because its quality of fusion is better than that of the outer layer and the structure of this layer is compact. There are hard phases (known from the above mentioned) in sub-surface layer and the structure of sub-surface layer is sound, which is the main contribution to the high hardness in this layer. The active atom decomposing from the melt of Ni-based alloying powder located in the most inner of preform diffuse into the substrate to form the transition layer with considerable thickness. The hard phase could not diffuse to this layer so that the content of hard phase drops obviously in this region. The Ni–Cr, Cu/Ni, Ni/Si solid solution and Ni–Cr–Fe alloy were the main composition at this layer, which is the main factor of micro-hardness falling obviously in this layer. Fig. 7 is the appearance of indentation at the Ni matrix. No cracking was concerned by the indentation, which indicates that the toughness is good though it was strengthened by hard phases.

4. Conclusion

Ni-based alloying powder and Al_2O_3 particulates with different content have been successfully used for fabricating surface composite on copper substrate by vacuum infiltration casting technology. The microstructure of infiltrated layer was compact. There was a transition layer between the surface composite Al_2O_3/Ni and substrate, which indicate that the surface composite has clearly excellent interfacial boundaries due to diffusion of elements across the interface, as apparent from their cross-sectional micrographs though the thickness of transition layer was different with different Al_2O_3 content.

The macro-hardness of infiltrated hardness reaches about HRC 65, and the average micro-hardness is around HV 700. The highest value of micro-hardness of surface composites increases somewhat with the increasing content of Al_2O_3. So the hardness of infiltrated layer has been improved markedly compared with the substrate.

Acknowledgements

The authors are pleased to acknowledge the financial support for this research provided by the National Natural Science Foundation of Gansu Project (ZS021-A25-024-C), the Chun-Hui Plan Project of the Ministry of Education of China (Z2004-1-62013) and Young Teacher Startup Foundation Project of Lanzhou University of Technology.

References

[1] K. Hyun-Ki, Surf. Coat. Technol. 190 (2005) 448–452.
[2] F. Findik, H. Uzum, Mater. Des. 24 (2003) 489–492.
[3] Z. Shi, M. Yan, Appl. Surf. Sci. 134 (1998) 103–106.
[4] S.-T. Oh, T. Sekino, K. Niihara, Nanostruct. Mater. 10 (1998) 715–722.
[5] P.G. Slade, IEEE Trans. Comp. Hybrids Manuf. Technol. 9 (1986) 3–11.
[6] O. Preston, N.J. Grant, AIME 221 (1961) 164–175.
[7] P. Bronsted, T.O. Sorensen, J. Mater. Sci. 13 (1978) 1224–1229.
[8] A. Upadhyyaya, G.S. Upadhyyaya, Mater. Des. 16 (1995) 41–45.
[9] D.Y. Ying, D.L. Zhang, Mater. Sci. Eng. A 226 (2000) 152–156.
[10] S. Sen, Surf. Coat. Technol. 190 (2005) 1–6.
[11] I. Ozbek, C. Bindal, Surf. Coat. Technol. 154 (2002) 14–20.
[12] B.S. Mann, Wear 208 (1997) 125–131.
[13] C. Bindal, A.H. Ucisik, J. Austr. Ceram. Soc. 34 (2) (1998) 287–292.
[14] S. DAS, P.P. Bandyopadhyay, T.K. Bandyopadhyay, S. Ghosh, A.B. Chattopadhyay, Metall. Mater. Transact. A34A (2003) 1909–1917.
[15] J. Lapin, D. Tiberghien, F. Delannay, Intermetallics 8 (2000) 1429–1438.
[16] S. Abraham, B.C. Pai, K.G. Satyanarayana, V.K. Vaidy, J. Mater. Sci. 25 (8) (1990) 2839–2846.
[17] K. Krishnaveni, T.S.N. Sankara Narayanan, S.K. Seshadri, Surf. Coat. Technol. 190 (2005) 115–121.
[18] R. Zhou, Y. Jiang, D. Lu, Wear 255 (1–6) (2003) 134–138.
[19] L.I. Zhen-xia, Nonferrous Metals Handbook, Mechanical Industrial Press, Beijing, 1978, p. 398–399.
[20] Y. Chen, DD.L. Chung, J. Mater. Sci. 31 (1996) 2117–2126.
[21] D.L. Joslin, D.S. Easton, C.T. Liu, S.S. Babu, S.A. David, Intermetallics 3 (1995) 467–481.
[22] D.C. Dunand, Mater. Manuf. Proc. 10 (1995) 373–381.
[23] H. Nakae, H. Fujii, K. Nakajima, A. Goto, Mater. Sci. Eng. A 223 (1997) 21–28.
[24] S. San Marchi, A. Mortensen, Metall. Mater. Trans. A 29 (1998) 2819–2829.
[25] H. Chen, M. Kaya, R.W. Smith, Materials 13 (1992) 180–193.
[26] D.L. Joslin, D.S. Easton, C.T. Liu, S.A. David, Mater. Sci. Eng. A 192/193 (1995) 544–548.